[Geophysical Research Letters]

Supporting Information for

New ocean subsurface optical properties from space lidars: CALIOP/CALIPSO and ATLAS/ICESat-2

X. Lu[1,2], Y. Hu[2], Y. Yang[3], T. Neumann[3], A. Omar[2], R. Baize[2], M. Vaughan[2], S. Rodier[1,2], B. Getzewich[2], Pat Lucker[1,2], Chip Trepte[2], C. Hostetler[2], and D. Winker[2]

[1]Science Systems and Applications, Inc., Hampton, VA, 23666, USA.

[2]NASA Langley Research Center, Hampton, VA, 23681, USA.

[3]NASA Goddard Space Flight Center, Greenbelt, MD, 20771, USA.

Contents of this file

Text S1: CALIOP data product and methods

The analysis and results presented in this work use CALIOP version 4 (V4) level 1 data products, in which the calibration of the measured attenuated backscatter coefficients at 532 nm were significantly improved (Getzewich et al., 2018; Kar et al., 2018). The CALIPSO V4.10 lidar level 1 data used in this study can be freely accessed via https://doi.org/10.5067/CALIOP/CALIPSO/ LID_L1-Standard-V4-10.

S1.1 Crosstalk calculation

The CALIOP backscatter signal at 532 nm is separated into parallel (∥) and perpendicular (⊥) components by a polarization beam splitter in the receiver subsystem (Hunt et al., 2009; Winker et al., 2009). With an ideal beam splitter, the measured molecular depolarization ratio (δ_{mol}) would equal the theoretical value of ~0.0035. As a result, the difference between the measured and theoretical molecular depolarization ratios indicates the level of crosstalk (*CT*) between the two polarization channels. The crosstalk represents the fraction of the optical power polarized parallel to the receiver polarization reference plane that is transferred to the perpendicular channel due to the non-ideal instrument effects (Chris A. Hostetler et al., 2006) as following:

$$\beta'_{\perp,measured} = \beta'_{\perp,true} + CT \times \beta'_{\perp,true} \quad (1)$$

$$\beta'_{\parallel,measured} = \beta'_{\parallel,true} - CT \times \beta'_{\parallel,true} \quad (2)$$

Here, we assume for simplicity that a fraction (CT) of $\beta'_{\parallel,true}$ is reflected into the perpendicular channel (Eq. 1) and that the remainder (1−CT) of the parallel signal $\beta'_{\parallel,true}$ is transmitted into the parallel detector (Eq. 2). With this assumption, the *CT* can be estimated as:

$$CT = \frac{\delta_{mol,measured}}{PGR} - 0.0035 \quad (3)$$

where PGR is the polarization gain ratio, which accounts for differences in the responsivity and gain of the two polarization channels at 532 nm and the relative transmission of the optics downstream of the polarizing beam splitter. The measured molecular depolarization ratio ($\delta_{mol,measured}$) is the ratio between $\beta'_{\perp,measured}$ and $\beta'_{\parallel,measured}$ at altitude region of 20 - 30 km where the measured signals are mostly from molecular backscatter and additional aerosol and cloud backscatter can be neglected.

For a linearly polarized incident lidar beam (e.g., CALIOP), spherical particles, Rayleigh scattering and reflection at the ocean surface do not contribute significantly to cross polarization. Cross-polarization signal (measured by the perpendicular channel) is dominated by backscattering of non-spherical particles, e.g., plankton and other non-spherical particles in the water, while the co-polarization signal measured by the parallel channel is mainly from the ocean surface reflection. Thus, the correlation between CALIOP parallel ($\beta'_{\parallel,true}$) and perpendicular ($\beta'_{\perp,true}$) signals should be minimum. The second method to estimate the crosstalk is using the measured signals over oceans. The *CT* is estimated when the correlation between ocean signals $\beta'_{\perp,measured} - CT \times \beta'_{\parallel,measured}$ and $\beta'_{\parallel,measured}$ is minimum. Compared with Eq. 3, the second method does not require the values of PGR, measured clean air depolarization ratio δ_{mol} and theoretical value of clean air depolarization ratio (0.0035 in Eq. 3).

Figure S1 shows the time series of crosstalk values calculated from CALIOP level 0 (daily mean) by Eq. 3 and from level 1 V4 data (monthly) by the second method from June 2006 to November 2020. The monthly crosstalk values are estimated over two chosen regions: 0º-40ºN (blue in Fig. S1), 0º-40ºS (pink in Fig. S1) during both daytime and nighttime. The relative differences of crosstalk values at the two chosen regions are less than 10%. The mean difference of crosstalk between day and night (Fig. S1(b)) is less than 5%.

S1.2 Effects of Crosstalk on measured ocean backscattered signals and its correction

Even though the crosstalk values are less than 1% over the CALIPSO entire mission (Fig. S1), its effects on ocean signals at perpendicular channel can be still large. For example, we assume the true ocean backscattered signals as: $\beta'_{\perp,true}$=1 and $\beta'_{\parallel,true} = 100$ with true depolarization ratio as 1% (e.g., Fig. S3). The crosstalk of 0.5% will cause the measured ocean signals as (Eq. 1 and 2): $\beta'_{\perp,measured} = 1.5$ and $\beta'_{\parallel,measured}$=99.5 with measured depolarization ratio as ~1.5%. The relative error ($\frac{\beta'_{\perp,measured}-\beta'_{\perp,true}}{\beta'_{\perp,true}} \times 100\%$) of measured perpendicular signal and depolarization ratio are ~50%. The effects of crosstalk can be up to 100% or more over ocean zones where the concentrations of phytoplankton are particularly low.

In summary, for the ocean backscattered signals with total depolarization ratio usually less than 0.1 (Fig. S3 and S4), the crosstalk can cause errors on the measured cross-polarized signals and should be corrected in order to get reliable ocean results. Briefly, the crosstalk-corrected signals ($\beta'_{\parallel,correct}, \beta'_{\perp,correct}$) can be derived from the measured signals as follows (Pitts et al., 2018):

$$\beta'_{\parallel,correct} = \beta'_{\parallel,measured}/(1 - CT) \quad (4)$$

$$\beta'_{\perp,correct} = \beta'_{\perp,measured} - CT \times \beta'_{\parallel,correct} \quad (5)$$

The new global cross-polarization component of ocean subsurface backscatter ($\gamma_\perp$, sr^{-1}) are obtained from CALIOP crosstalk-corrected ocean attenuated backscatter coefficients $\beta'_{\parallel,correct}$ and $\beta'_{\perp,correct}$ as:

$$\gamma_\perp = \frac{\int_{p-1}^{p+3} \beta'_{\perp,correct}}{T^2_{atm}} \quad (6)$$

$$T^2_{atm} = \frac{\gamma_\parallel}{\beta_s} = \frac{\int_{p-1}^{p+3} \beta'_{\parallel,correct}}{\beta_s} \quad (7)$$

where p indicates the peak ocean surface return bin and β_s is the theoretical ocean surface backscatter estimated from wind speed (Hu et al., 2008). The AMSR-E (2006-2011) and Modern-Era Retrospective Analysis for Research and Applications-version 2 (MERRA-2) (2011-2020) wind speed are used in this paper.

The seasonal changes of CALIOP total depolarization ratio ($\delta_t = \frac{\gamma_\perp}{\gamma_\parallel}$) at nighttime (Fig. S3) and daytime (Fig. S4) are crosstalk corrected ratios. Data are seasonally averaged climatologies for the 2008-2020 period binned to 1º latitude × 1º longitude pixels.

Text S2: ICESat-2 data product and methods

The analysis and results presented in this work use ICESat-2 geolocated photon data (ATL03 Release 003), which are publicly available through National Snow and Ice Data Center (NSIDC) (Neumann et al., 2020).

S2.1 ATLAS/ICESat-2 after pulsing effects and its correction

The afterpulses are typically present in the ICESat-2 measured photon events after almost any surface returns, but are most easily seen beneath strong surface returns from highly reflective surfaces such as smooth sea ice. Figure S5 shows ICESat-2 photon heights from (a) land, (b) ocean, (c) sea ice, and (d) land ice surfaces along selected ICESat-2 ground tracks. The blue dots represent all photon events between likely background photon events and likely signal photon events, and the red dots indicate those signal photon events having high confidence levels. The high confidence photons are most likely backscattered from the Earth's surface. The afterpulses can be clearly seen blow primary surfaces as indicated in Fig. S5.

The magnitude of afterpulses can be the same order of magnitude as the ocean subsurface signals as indicated in Fig. S5(b). Therefore, the ICESat-2 ATLAS after-pulsing effects must first be removed in order to obtain a more accurate ocean subsurface profile. A deconvolution method describe in (Lu et al., 2014; Lu, Hu, Vaughan, et al., 2020; Lu, Hu, Yang, et al., 2020) can be used to remove the ICESat-2 ATLAS afterpulses.

Figure S6 gives the concept and schematic flow chart of applying ICESat-2 ATL03 data for ocean subsurface optical properties retrieval (Lu, Hu, Yang, et al., 2020).

Figure S7 shows the ICESat-2 ground tracks (blue and black) from which the photons studied in this paper were harvested. The blue represents ground tracks on March 5th, 2019 and the black stands for ground tracks over Indian ocean with reference ground track (RGT) number of 0280. The ATLAS ATL03 data from October 2018 to July 2020 (Table S1) with RGT number of 0280 are used in this study.

The two-dimensional distributions of (a) attenuated backscatter coefficient ($\beta(z)$, m^{-1}sr^{-1}) and (b) total backscattering coefficient ($b_b(z)$) obtained from ICESat-2 measurement over Indian ocean (black line in Fig. S5) on April 13th, 2020 are given in Fig. S8 for example. The corresponding ICESat-2 derived diffuse attenuation coefficient, kd (m^{-1}), layer integrated subsurface attenuated backscatter (Rrs, sr^{-1}) and b_b (m^{-1}) are compared with MODIS results (Fig. S9). The relationships between ICESat-2 derived ocean results and MODIS ocean color results over Indian ocean with RGT #0280 from October 2018 to July 2020 are present in Fig. S10, with the corresponding statistics of relative differences given in Table S1. The results indicate the relative differences between ICESat-2 and MODIS are ~11%, 10% and 27% for kd, b_b and Rrs, respectively. These differences are mainly due to the time offset and the different measurement locations (up to 10 km) between ICESat-2 (daily) and MODIS (monthly). Moreover, MERRA-2 wind speed is used to calibrate ICESat-2 observed photons from ocean surface (Hu et al., 2008; Lu, Hu, Yang, et al., 2020). The calibration accuracy depends on the accuracy of the MERRA-2 wind speed, which is beyond the scope of this study.

Text S3: MODIS ocean color data and methods

Because there are not many daily measurements co-located with ATLAS/ICESat-2 measurements, MODIS-Aqua monthly ocean color results (NASA, 2018) are used in this

work. The MODIS diffuse attenuation coefficient, kd (m^{-1}) at 490 nm was scaled to 532 nm as (Lu et al., 2016): $Kd_{532} = 0.68(Kd_{490} - 0.022) + 0.054$. The MODIS remote sensing reflectance (Rrs, sr^{-1}) data at 531 nm and total backscattering coefficient (b_b, m^{-1}) at 531 nm by the Generalized Inherent Optical Property (GIOP) model (Werdell, Franz, Bailey, et al., 2013) are used in this paper. The MODIS kd, b_b and Rrs data product can be freely downloaded from NASA Ocean Color Data Web (http://oceandata.sci.gsfc.nasa.gov accessed on 03/23/2021).

Figure S2 shows the seasonal distribution of remote sensing reflectance at 531 nm from MODIS measurements. Data are seasonally averaged climatologies for the 2008-2020 period binned to 1º latitude × 1º longitude pixels.

Text S4: Argo float profiling data and methods

Biogeochemical-Argo is a network of profiling floats carrying bio-optical sensors which can measure vertical profiles of temperature, salinity, pressure, chlorophyll a concentration and particle backscattering coefficient (b_{bp}, m^{-1}) at 700 nm (Organelli et al., 2017). This Biogeochemical-Argo network represents today's most promising strategy for collecting temporally and vertically resolved observations of biogeochemical properties throughout the ocean. The Argo network has already delivered extensive high-quality global data sets that have resulted in unique scientific outcomes from regional to global scales. The Argo floats data are freely available at http://www.coriolis.eu.org/Data-Products/Data-Delivery/Data-selection.

The Argo float profiles at (9.32ºS, 141ºW) on March 5th, 2019 were used in this study (red in Fig. S7). The corresponding Argo float's temperature and salinity profiles are used to estimate the seawater backscattering coefficient profile (b_{bw}, m^{-1}) at 532 nm by method in (Werdell, Franz, Lefler, et al., 2013). To match ICESat-2 results at 532 nm, Argo float b_{bp} results at 700 nm were scaled to 532 nm according to: $b_{bp}(532) = b_{bp}(700) \times (\frac{700}{532})^{\eta}$, where the power-law slope (η) can vary from 0 to 4.3 (Maritorena et al., 2002). For the Argo data on March 5th, 2019, η is selected as 2. The relative differences of b_{bp} at 532 nm between $\eta = 1$ and $\eta = 2$ are ~24%.

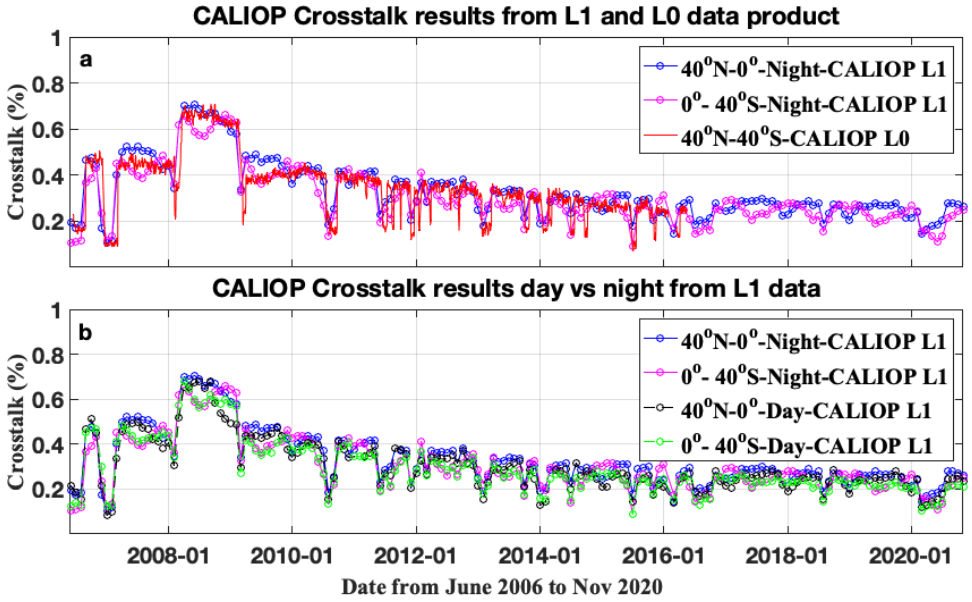

Figure S1. Time series of crosstalk calculated from CALIOP level 0 (Eq. 3) daily and level 1 V4 monthly data (June 2006 to November 2020).

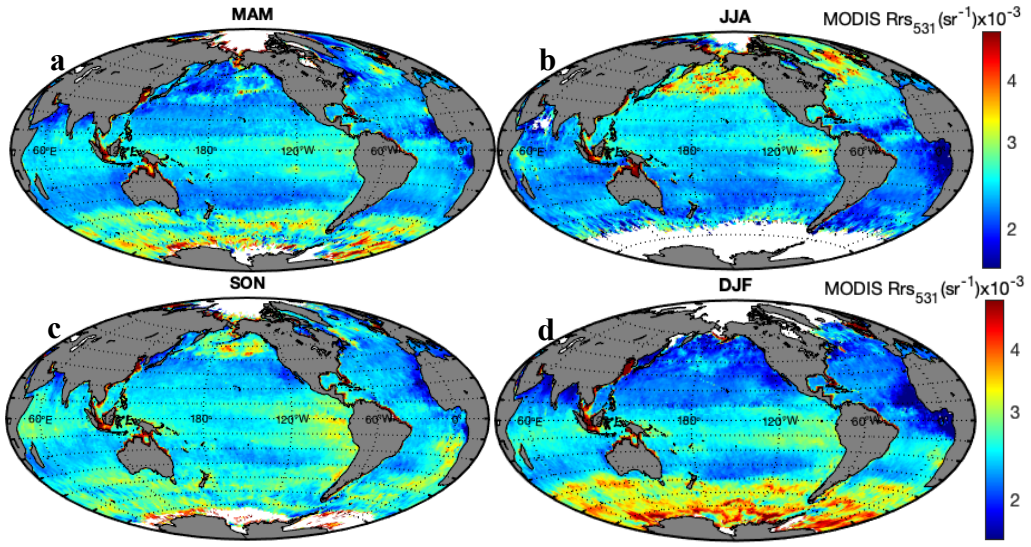

Figure S2. Seasonal changes of MODIS remote sensing reflectance (Rrs, sr^{-1}) during daytime: (a) March - May; (b) June - August; (c) September - November; (d) December - February. Data are seasonally averaged climatologies for the 2008-2020 period binned to 1º latitude × 1º longitude pixels.

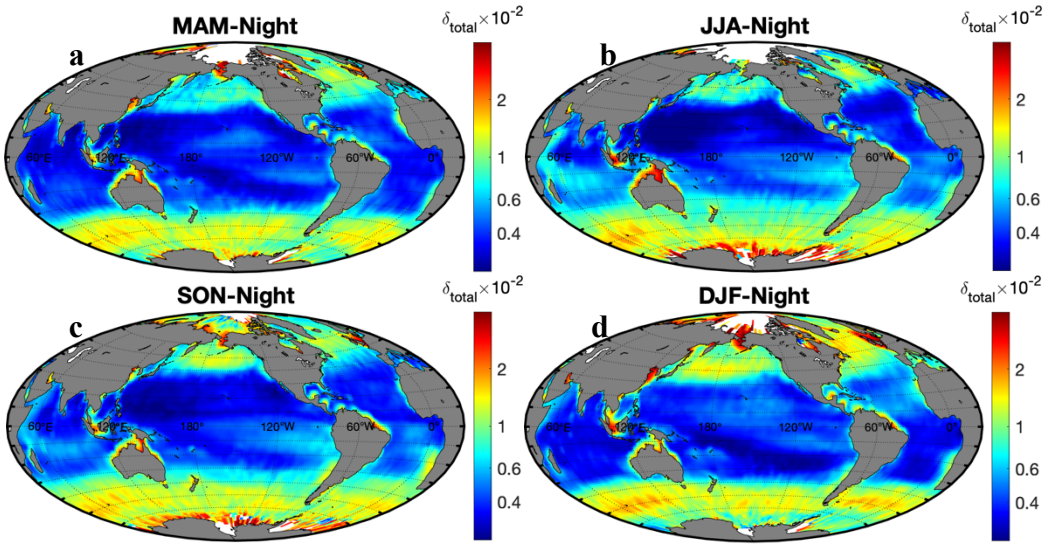

Figure S3. Seasonal changes of CALIOP total depolarization ratio (δ_t) at nighttime. (a) March - May; (b) June - August; (c) September - November; (d) December - February. Data are seasonally averaged climatologies for the 2008-2020 period and have been averaged to 1º latitude × 1º longitude pixels.

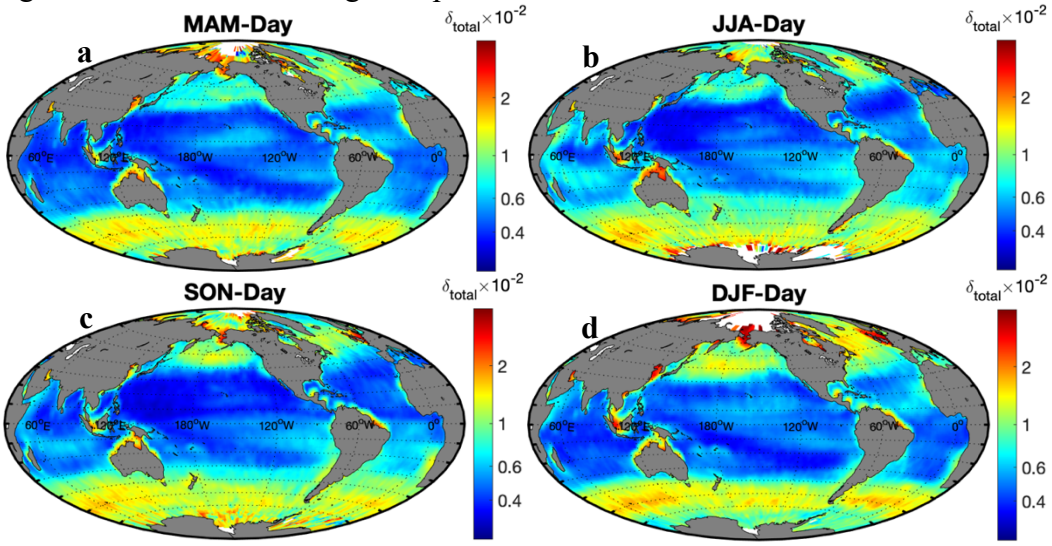

Figure S4. Same with Fig. S2 but for daytime total depolarization ratio.

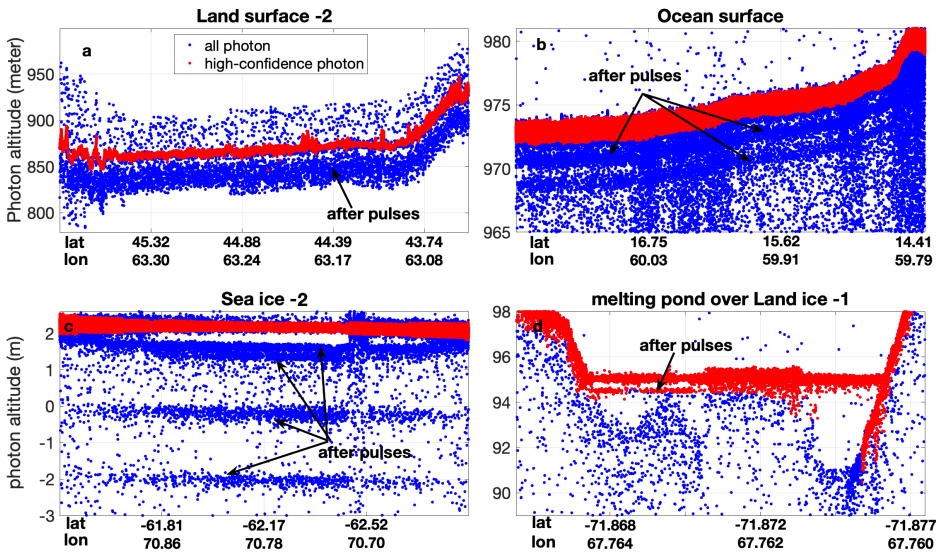

Figure S5. ICESat-2 after pulses found in photon events. From Figure 1 of reference Lu et.al., 2021.

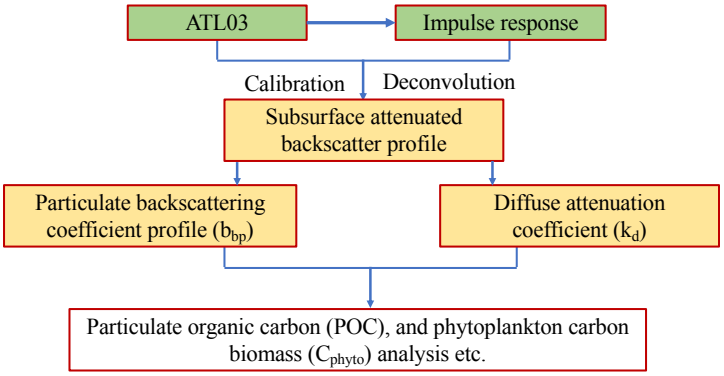

Figure S6. Concept and schematic flow chart of applying ICESat-2 ATL03 data for ocean subsurface optical properties retrievals (Lu, Hu, Yang, et al., 2020).

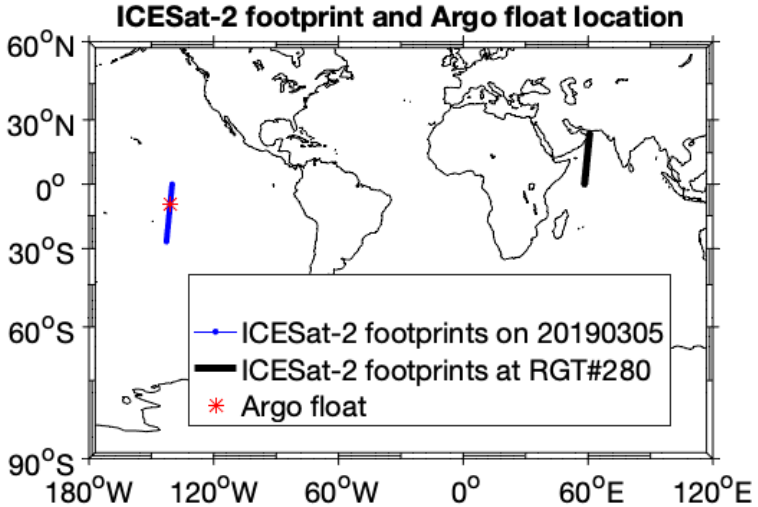

Figure S7. ICESat-2 ground tracks (blue and black) from which the photons studied in this paper were harvested. The blue represents ground tracks on March 5th, 2019 and the black

stands for ground tracks over Indian ocean with RGT # 0280 from October 2018 to July 2020 (Table S1). The red indicates the location of Argo float data on March 5th, 2019 used in this paper.

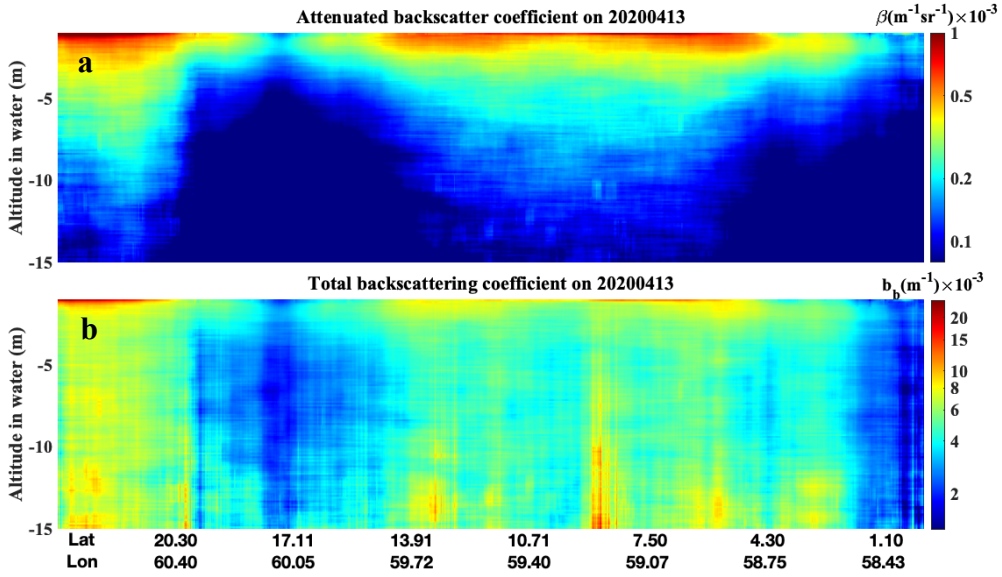

Figure S8. Two-dimensional distributions of (a) attenuated backscatter coefficient (β, $m^{-1}sr^{-1}$) and (b) total backscattering coefficient below ocean surface (b_b, m^{-1}) on April 13th 2020. The x-axis specifies locations along ICESat-2 ground tracks (black line in Fig. S5) and y-axis is ocean penetration depth in meters. The color bars on the right-hand side provide the range of β and b_b values.

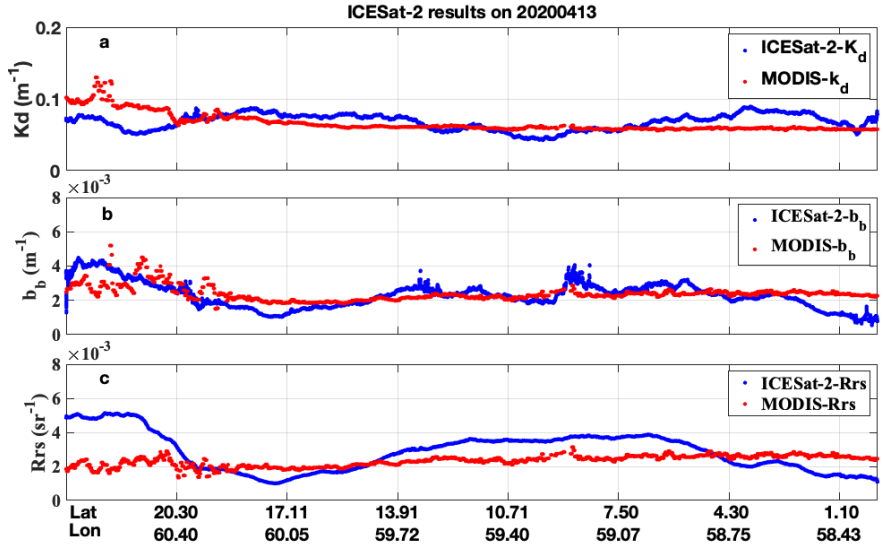

Figure S9. Comparison between ICESat-2 results om April 13th 2020 (blue) and co-located MODIS monthly results in April 2020 (red). (a) diffuse attenuation coefficient, *kd* (m^{-1}); (b) layer-integrated total backscattering coefficient, b_b (m^{-1}); (c) layer-integrated ocean subsurface attenuated backscatter (sr^{-1}).

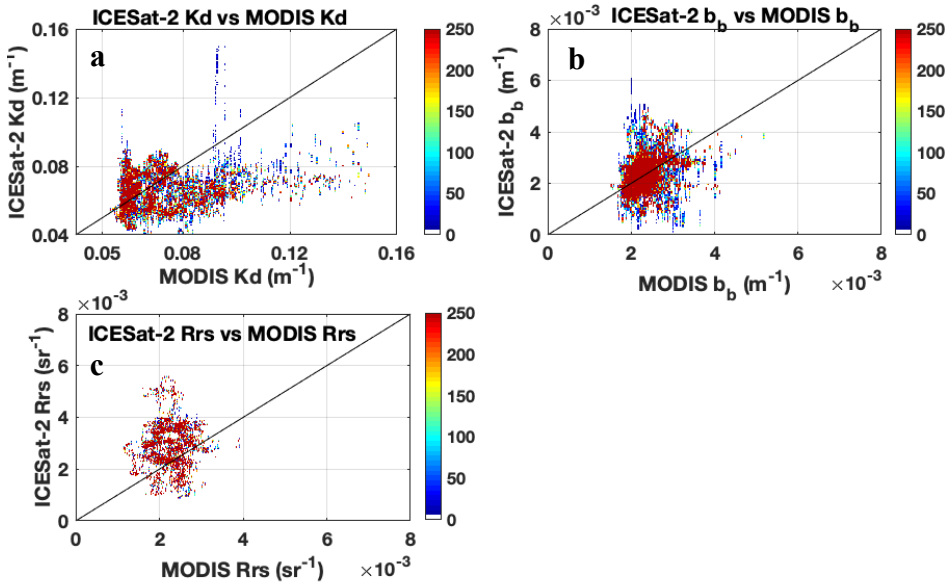

Figure S10. Comparisons between ICESat-2 and MODIS ocean results, where the ICESat-2 results are over Indian Ocean (black in Fig. S5) with RGT # 0280 from October 2018 to July 2020 (Table S1). The color on right-hand side indicates the number of ICESat-2 profiles co-located with MODIS monthly ocean color results.

Table S1. Relative differences between ICESat-2 and MODIS ocean results over Indian Ocean (black line in Fig. S5) for different cycles (times). The ICESat-2 Reference Ground Track (RGT) number is 0280.

Time	*Kd* (m^{-1})	b_b (m^{-1})	*Rrs* (sr^{-1})
2018-10-16	~11%	~3%	~20%
2019-01-15	~29%	~12%	~31%
2019-04-16	~4%	~11%	~9%
2020-01-14	~19%	~20%	~51%
2020-04-13	~7%	~4%	~22%
2020-07-13	~13%	~9%	~26%
Mean	~11%	~10%	~27%